Relative Dynamics including J2 Effects

ASTRO 6579

Michael Wang , mw732
Mitchell Dominguez, md697
May 9, 2018

LVLH Frame Kinematics

Given the Earth-Centered-Inertial (ECI) frame $\mathcal{I} = (\mathcal{O}, \boldsymbol{e_1}, \boldsymbol{e_2}, \boldsymbol{e_3})$, the Local-Vertical-Local-Horizontal (LVLH) frame $\mathcal{B} = (\mathcal{C}, \hat{\boldsymbol{x}}, \hat{\boldsymbol{y}}, \hat{\boldsymbol{z}})$ is defined as:

$$\hat{\boldsymbol{x}} = \frac{\boldsymbol{r}}{r} \qquad \hat{\boldsymbol{y}} = \hat{\boldsymbol{z}} \times \hat{\boldsymbol{x}} \qquad \hat{\boldsymbol{z}} = \frac{\boldsymbol{h}}{h} \tag{1}$$

where $\boldsymbol{r}$ is the position vector and $\boldsymbol{h}$ is the angular momentum vector of the reference orbit. The position vector can be expressed in terms of both LVLH and ECI coordinates as follows:

$$\boldsymbol{r} = r\hat{\boldsymbol{x}} = X\boldsymbol{e_1} + Y\boldsymbol{e_2} + Z\boldsymbol{e_3} \tag{2}$$

The rotation matrix from ECI to LVLH frame can be expressed as an Euler angle set (3-1-3):

$$\begin{aligned} {}^{\mathcal{I}}R^{\mathcal{B}} &= R_{\Omega,3}R_{I,1}R_{\theta,3} \\ &= \begin{bmatrix} c(\Omega) & -s(\Omega) & 0 \\ s(\Omega) & c(\Omega) & 0 \\ 0 & 0 & 1 \end{bmatrix} \begin{bmatrix} 1 & 0 & 0 \\ 0 & c(I) & -s(I) \\ 0 & s(I) & c(I) \end{bmatrix} \begin{bmatrix} c(\theta) & -s(\theta) & 0 \\ s(\theta) & c(\theta) & 0 \\ 0 & 0 & 1 \end{bmatrix} \\ &= \begin{bmatrix} c(\Omega)c(\theta) - c(I)s(\Omega)s(\theta) & -c(\Omega)s(\theta) - c(I)s(\Omega)c(\theta) & s(I)s(\Omega) \\ s(\Omega)c(\theta) + c(I)c(\Omega)s(\theta) & c(I)c(\Omega)c(\theta) - s(\Omega)s(\theta) & -c(\Omega)s(I) \\ s(I)s(\theta) & s(I)c(\theta) & c(I) \end{bmatrix} \end{aligned} \tag{3}$$

where $\theta = \nu + \omega$. The angular velocity vector of LVLH frame with respect to ECI frame can be calculated as:

$$\begin{aligned} \boldsymbol{\omega}^{\mathcal{B}/\mathcal{I}} \triangleq \begin{bmatrix} \omega_x \\ \omega_y \\ \omega_z \end{bmatrix}_{\mathcal{B}} &= R_{\theta,3}^T R_{I,1}^T \begin{bmatrix} 0 \\ 0 \\ \dot{\Omega} \end{bmatrix} + R_{\theta,3}^T \begin{bmatrix} \dot{I} \\ 0 \\ 0 \end{bmatrix} + \begin{bmatrix} 0 \\ 0 \\ \dot{\theta} \end{bmatrix} \\ &= \begin{bmatrix} \dot{I}c(\theta) + \dot{\Omega}s(I)s(\theta) \\ \dot{\Omega}s(I)c(\theta) - \dot{I}s(\theta) \\ \dot{\theta} + \dot{\Omega}c(I) \end{bmatrix}_{\mathcal{B}} \end{aligned} \tag{4}$$

Using definitions from Equation 1, we can find the time derivative of the position vector using the transport theorem:

$$\dot{\boldsymbol{r}} = \frac{{}^{\mathcal{I}}d}{dt}(r\hat{\boldsymbol{x}}) = \dot{r}\hat{\boldsymbol{x}} + r\boldsymbol{\omega}^{\mathcal{B}/\mathcal{I}} \times \hat{\boldsymbol{x}} = \dot{r}\hat{\boldsymbol{x}} + \frac{h}{r}\hat{\boldsymbol{y}} \tag{5}$$

The angular momentum vector can be calculated as:

$$\boldsymbol{h} = \boldsymbol{r} \times \dot{\boldsymbol{r}} = \begin{bmatrix} 0 \\ r^2\omega_y \\ r^2\omega_z \end{bmatrix}_{\mathcal{B}} \tag{6}$$

According to Equation 1, $\hat{\boldsymbol{z}} = \frac{\boldsymbol{h}}{h}$. This means $\boldsymbol{h} \parallel \hat{\boldsymbol{z}}$ and $\omega_y = 0$. Thus, we have:

$$\omega_z = \frac{h}{r^2} \tag{7}$$

and the time derivative of the LVLH unit vectors are then:

$$\dot{\hat{\boldsymbol{x}}} = \boldsymbol{\omega}^{\mathcal{B}/\mathcal{I}} \times \hat{\boldsymbol{x}} = \omega_z\hat{\boldsymbol{y}} \qquad \dot{\hat{\boldsymbol{y}}} = \boldsymbol{\omega}^{\mathcal{B}/\mathcal{I}} \times \hat{\boldsymbol{y}} = \omega_x\hat{\boldsymbol{z}} - \omega_z\hat{\boldsymbol{x}} \qquad \dot{\hat{\boldsymbol{z}}} = \boldsymbol{\omega}^{\mathcal{B}/\mathcal{I}} \times \hat{\boldsymbol{z}} = -\omega_x\hat{\boldsymbol{y}} \tag{8}$$

Reference Satellite Dynamics in LVLH Frame

The governing equation of the reference satellite S_0 is given by:

$$\ddot{\boldsymbol{r}} = -\nabla U \tag{9}$$

where the double time derivative of the position vector can be computed using Equation 5:

$$\begin{aligned}\ddot{\boldsymbol{r}} &= \ddot{r}\hat{\boldsymbol{x}} + \dot{r}\frac{h}{r^2}\hat{\boldsymbol{y}} + \frac{r\dot{h} - h\dot{r}}{r^2}\hat{\boldsymbol{y}} - \frac{h^2}{r^3}\hat{\boldsymbol{x}} + \omega_x\frac{h}{r}\hat{\boldsymbol{z}} \\ &= \left(\ddot{r} - \frac{h^2}{r^3}\right)\hat{\boldsymbol{x}} + \frac{\dot{h}}{r}\hat{\boldsymbol{y}} + \frac{\omega_x h}{r}\hat{\boldsymbol{z}}\end{aligned} \tag{10}$$

and where the potential, U, contains the Kepler term and the oblateness term:

$$U = -\frac{\mu}{r} - \frac{3J_2\mu R_e^2}{2r^3}\left(\frac{1}{3} - s^2(\phi)\right) \tag{11}$$

Defining the following constant:

$$k_{J2} = \frac{3J_2\mu R_e^2}{2} \tag{12}$$

Equation 11 can be simplified to

$$U = -\frac{\mu}{r} - \frac{k_{J2}}{r^3}\left(\frac{1}{3} - s^2(\phi)\right) \tag{13}$$

The gradient of U is defined as:

$$\nabla U = \frac{\partial U}{\partial X}\boldsymbol{e_1} + \frac{\partial U}{\partial Y}\boldsymbol{e_2} + \frac{\partial U}{\partial Z}\boldsymbol{e_3} \tag{14}$$

Taking each of the partial derivatives in Equation 14:

$$\begin{aligned}\frac{\partial U}{\partial X} &= \frac{\mu X}{r^3} + \frac{k_{J2}X}{r^5} - \frac{5k_{J2}Z^2X}{r^7} \\ \frac{\partial U}{\partial Y} &= \frac{\mu Y}{r^3} + \frac{k_{J2}Y}{r^5} - \frac{5k_{J2}Z^2Y}{r^7} \\ \frac{\partial U}{\partial Z} &= \frac{\mu Z}{r^3} + \frac{k_{J2}Z}{r^5} + k_{J2}\frac{2Zr^2 - 5Z^3}{r^7}\end{aligned} \tag{15}$$

Equations 15 can be simplified by using the geocentric latitude ϕ, which is measured from the $\boldsymbol{e_1} - \boldsymbol{e_2}$ plane to the position vector. By also taking the Z-component of ${}^{\mathcal{I}}R^{\mathcal{B}}[\boldsymbol{r}]_{\mathcal{B}}$, ϕ can be expressed as shown below:

$$s(\phi) = \frac{Z}{r} = s(I)s(\theta) \tag{16}$$

Using the above definition, the gradient of U can be simplified to the following form:

$$\begin{aligned}\frac{\partial U}{\partial X} &= \frac{\mu X}{r^3} + \frac{k_{J2}X}{r^5}\left(1 - 5s^2(\phi)\right) \\ \frac{\partial U}{\partial Y} &= \frac{\mu Y}{r^3} + \frac{k_{J2}Y}{r^5}\left(1 - 5s^2(\phi)\right) \\ \frac{\partial U}{\partial Z} &= \frac{\mu Z}{r^3} + \frac{k_{J2}Z}{r^5}\left(1 - 5s^2(\phi)\right) + \frac{2k_{J2}s(\phi)}{r^4}\end{aligned} \tag{17}$$

Using the above developments and using the definition of $\boldsymbol{r}$ in ECI coordinates, ∇U can be written as:

$$\nabla U = \left(\frac{\mu}{r^2} + \frac{k_{J2}}{r^4} \left(1 - 5s^2(\phi)\right) \right) \hat{\boldsymbol{r}} + \frac{2k_{J2}s(\phi)}{r^4} \hat{\boldsymbol{Z}} \tag{18}$$

Equation 18 can be expressed in LVLH frame coordinates by using the following equations:

$$\begin{aligned} \hat{\boldsymbol{Z}} &= s(\theta)s(I)\hat{\boldsymbol{x}} + c(\theta)s(I)\hat{\boldsymbol{y}} + c(I)\hat{\boldsymbol{z}} \\ s(\phi) &= s(\theta)s(I) \\ \hat{\boldsymbol{r}} &= \hat{\boldsymbol{x}} \end{aligned} \tag{19}$$

Applying the above equations, ∇U is as follows

$$\nabla U = \left(\frac{\mu}{r^2} + \frac{k_{J2}}{r^4} \left(1 - 3s^2(I)s^2(\theta)\right) \right) \hat{\boldsymbol{x}} + \frac{k_{J2}s^2(I)s(2\theta)}{r^4} \hat{\boldsymbol{y}} + \frac{k_{J2}s(2I)s(\theta)}{r^4} \hat{\boldsymbol{z}} \tag{20}$$

Using our expressions for $\ddot{\boldsymbol{r}}$ and ∇U and applying Equation 9, the first three of six scalar equations of motion for the reference satellite can be obtained:

$$\begin{aligned} \dot{r} &= v_x \\ v_x = \ddot{r} &= \frac{h^2}{r^3} - \frac{\mu}{r^2} - \frac{k_{J2}}{r^4} \left(1 - 3s^2(I)s^2(\theta)\right) \\ \dot{h} &= -\frac{k_{J2}s^2(I)s(2\theta)}{r^3} \end{aligned} \tag{21}$$

Additionally, an equation for ω_x is found through this method:

$$\omega_x = -\frac{k_{J2}s(\theta)s(2I)}{hr^3} \tag{22}$$

Using Equations 4, 7, and 22, the last three scalar equations of motion for the satellite can be found as such:

$$\begin{aligned} \dot{\Omega} &= -\frac{2k_{J2}s^2(\theta)c(i)}{hr^3} \\ \dot{I} &= -\frac{k_{J2}s(2I)s(2\theta)}{2hr^3} \\ \dot{\theta} &= \frac{h}{r^2} + \frac{2k_{J2}s^2(\theta)c^2(I)}{hr^3} \end{aligned} \tag{23}$$

Equations 21 and 23 fully describe the motion of the reference satellite under J_2 perturbations. By taking the time derivative of Equation 7 and using the relation in Equation 21, we get the following:

$$\alpha_z = \dot{\omega}_z = \frac{r^2\dot{h} - 2hr\dot{r}}{r^4} = -\frac{2h\dot{r}}{r^3} - \frac{k_{J2}s^2(I)s(2\theta)}{r^5} \tag{24}$$

Taking the time derivative of ω_x, and using Equations 21 to 23, we get the following:

$$\alpha_x = \dot{\omega}_x = -\frac{k_{J2}s(2I)c(\theta)}{r^5} + \frac{3\dot{r}k_{J2}s(2I)s(\theta)}{r^4h} - \frac{8k_{J2}^2s^3(I)c(I)s^2(\theta)c(\theta)}{r^6h^2} \tag{25}$$

Exact Nonlinear J_2 Relative Dynamics

The dynamics of each member satellite S_j of the formation are derived with respect to the reference satellite S_0. Figure 1 demonstrates the geometry of the problem.

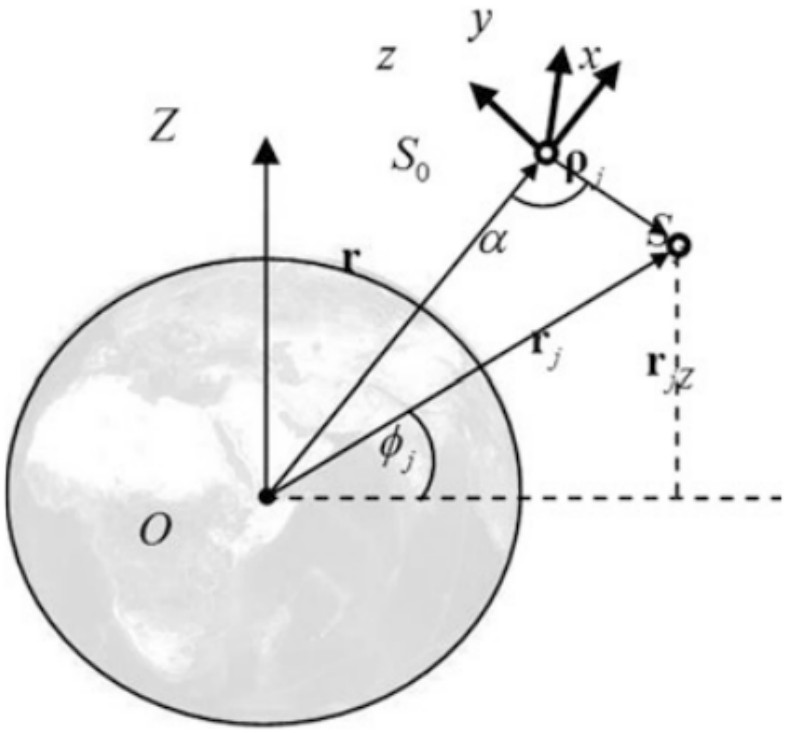

Figure 1: Geometry of the follower satellite [1]

The position and velocity of the member satellite relative to the center of the Earth is given as:

$$\begin{aligned}
\boldsymbol{r}_j &= \boldsymbol{r} + \boldsymbol{\rho}_j = r\hat{\boldsymbol{x}} + (x_j\hat{\boldsymbol{x}} + y_j\hat{\boldsymbol{y}} + z_j\hat{\boldsymbol{z}}) \\
\boldsymbol{r}_j &= (r + x_j)\hat{\boldsymbol{x}} + y_j\hat{\boldsymbol{y}} + z_j\hat{\boldsymbol{z}} \\
\dot{\boldsymbol{r}}_{\boldsymbol{j}} &= (\dot{r} + \dot{x}_j - y_j\omega_z)\hat{\boldsymbol{x}} + ((r + x_j)\omega_z + \dot{y}_j - z_j\omega_x)\,\hat{\boldsymbol{y}} + (y_j\omega_x + \dot{z}_j)\hat{\boldsymbol{z}}
\end{aligned} \tag{26}$$

The relative dynamics of the member satellites S_j with respect to the reference satellite S_0 can then be derived using the Lagrange formulation, which is defined below:

$$\frac{d}{dt}\left(\frac{\partial L_j}{\partial \dot{\boldsymbol{q}}_j}\right) - \frac{\partial L_j}{\partial \boldsymbol{q}_j} = \boldsymbol{F}_j \tag{27}$$

where $L_j = K_j - U_j$ is the Lagrangian of the member satellite, $\boldsymbol{q}_j = [x_j \quad y_j \quad z_j]^T$ is the configuration of the member satellite, and $\boldsymbol{F}_j = [F_{jx} \quad F_{jy} \quad F_{jz}]^T$ are the nonconservative

forces acting on the member satellite. $\boldsymbol{F}_j$ includes forces including control inputs as well as nonconservative perturbations like air drag or radiation pressure.

Equation 27 can be simplified slightly by applying the fact that while K_j depends on both the position and velocity of the member satellite, U_j only depends on position. Additionally, this paper does not account for nonconservative forces or control inputs. Therefore, $\boldsymbol{F}_j = \boldsymbol{0}$. Thus, the Lagrangian formulation simplifies down to the following:

$$\frac{d}{dt}\left(\frac{\partial K_j}{\partial \dot{\boldsymbol{q}}_j}\right) - \frac{\partial K_j}{\partial \boldsymbol{q}_j} + \frac{\partial U_j}{\partial \boldsymbol{q}_j} = \boldsymbol{0} \tag{28}$$

The kinetic energy $K_j = \frac{1}{2}\dot{\boldsymbol{r}}_j \cdot \dot{\boldsymbol{r}}_j$ of the member satellite is given by:

$$K_j = \frac{1}{2}(\dot{x}_j + v_x - y_j\omega_z)^2 + \frac{1}{2}\left(\dot{y}_j + (r + x_j)\omega_z - z_j\omega_x\right)^2 + \frac{1}{2}(\dot{z}_j + y_j\omega_x)^2 \tag{29}$$

and the potential energy U_j is given by

$$U_j = -\frac{\mu}{r_j} - \frac{k_{J2}}{r_j^3}\left(\frac{1}{3} - s^2(\phi_j)\right) \tag{30}$$

where ϕ_j is the geocentric latitude of the member satellite and r_j is the magnitude of the vector $\boldsymbol{r_j}$. The sine of the geocentric latitude in Equation 30 leads to the following:

$$s(\phi_j) = \frac{r_{jZ}}{r_j} \tag{31}$$

where

$$r_{jZ} = \boldsymbol{r_j} \cdot \hat{\boldsymbol{Z}} = (r + x_j)s(I)s(\theta) + y_j s(I)c(\theta) + z_j c(I) \tag{32}$$

Using Equations 31 and 32, U_j can be expressed as:

$$U_j = -\frac{\mu}{r_j} - \frac{k_{J_2}}{3r_j^3} + \frac{k_{J2}r_{jZ}^2}{r_j^5} \tag{33}$$

Given Equation 29, computing $\frac{\partial K_j}{\partial \boldsymbol{q}_j}$ and $\frac{\partial K_j}{\partial \dot{\boldsymbol{q}}_j}$ is straightforward partial differentiation. The tricky part comes when evaluating the time derivative of $\frac{\partial K_j}{\partial \dot{\boldsymbol{q}}_j}$. The multivariate chain rule can be used to compute the following quantity:

$$\frac{d}{dt}\left(\frac{\partial K_j}{\partial \dot{\boldsymbol{q}}_j}\right) = \frac{\partial}{\partial \boldsymbol{q}_j}\left(\frac{\partial K_j}{\partial \dot{\boldsymbol{q}}_j}\right)\dot{\boldsymbol{q}}_j + \left(\frac{\partial^2 K_j}{\partial \dot{\boldsymbol{q}}_j^2}\right)\ddot{\boldsymbol{q}}_j \tag{34}$$

Solving for the second time derivatives $\ddot{x}_j$, $\ddot{y}_j$, and $\ddot{z}_j$, the full nonlinear equations of motion of the follower satellite S_j can be obtained

$$\begin{aligned}
\ddot{x}_j &= 2\dot{y}_j\omega_z - x_j(\eta_j^2 - \omega_z^2) + y_j\alpha_z - z_j\omega_x\omega_z - (\zeta_j - \zeta)s(I)s(\theta) - r(\eta_j^2 - \eta^2) \\
\ddot{y}_j &= -2\dot{x}_j\omega_z + 2\dot{z}_j\omega_x - x_j\alpha_z - y_j(\eta_j^2 - \omega_z^2 - \omega_x^2) + z_j\alpha_x - (\zeta_j - \zeta)s(I)c(\theta) \\
\ddot{z}_j &= -2\dot{y}_j\omega_x - x_j\omega_x\omega_z - y_j\alpha_x - z_j(\eta_j^2 - \omega_x^2) - (\zeta_j - \zeta)c(I)
\end{aligned} \tag{35}$$

where ζ, η^2, ζ_j, and η_j^2 are terms introduced to simplify Equation 35 and that defined below:

$$\begin{aligned} \zeta &= \frac{2k_{J2}s(I)s(\theta)}{r^4} \\ \eta^2 &= \frac{\mu}{r^3} + \frac{k_{J2}}{r^5} - \frac{5k_{J2}s^2(I)s^2(\theta)}{r^5} \end{aligned} \tag{36}$$

$$\begin{aligned} \zeta_j &= \frac{2k_{J2}r_{jZ}}{r_j^5} \\ \eta_j^2 &= \frac{\mu}{r_j^3} + \frac{k_{J2}}{r_j^5} - \frac{5k_{J2}r_{jZ}^2}{r_j^7} \end{aligned} \tag{37}$$

Linearization

While the full J_2 equations of motion for the follower satellite dynamics are excellent for creating accurate simulations of satellite formations, the nonlinearities make designing control systems more difficult. Additionally, nonlinear systems are significantly more difficult to comprehend than linear systems. Thus, a linearization of the full J_2 dynamics is sought.

The terms ζ_j and η_j^2 as defined in (37) are nonlinear because they include higher order terms of $1/r_j$. To linearize these terms, Figure 1 and the law of cosines is used to obtain the following equations:

$$r_j^2 - r^2 - 2r\rho_j \cos\alpha + \rho_j^2 \tag{38}$$

where

$$\cos\alpha = \frac{(-\boldsymbol{r}) \cdot \boldsymbol{\rho_j}}{r\rho_j} = \frac{-x_j}{\rho_j} \tag{39}$$

Now, the Gebenbauer polynomials, as defined in Equation 40, can be used to obtain expressions for powers of $1/r_j$ in terms of r and x_j. In Equation 40, $\Gamma(n) = (n-1)!$.

$$C_n^{(\lambda)}(u) = \frac{\Gamma(\lambda + 1/2)}{\Gamma(2\lambda)} \frac{\Gamma(n+2\lambda)}{\Gamma(n+\lambda+1/2)} \frac{(-1)^n}{2^n n!} (1-u^2)^{-\lambda+1/2} \frac{d^n}{du^n} (1-u^2)^{n+\lambda-1/2} \tag{40}$$

The first two terms of Equation 40, where $n = 0$ and $n = 1$, are then as follows:

$$\begin{aligned} C_0^{(\lambda)}(u) &= 1 \\ C_1^{(\lambda)}(u) &= 2\lambda u \end{aligned} \tag{41}$$

If $(\lambda + 1/2) > 0$, $|v| < 1$, and $|u| \leq 1$, then the generating function of the Gebenbauer polynomials is as follows:

$$(1 - 2uv + v^2)^{-\lambda} = \sum_{n=0}^{\infty} C_n^{(\lambda)}(u) v^n \approx 1 + (2\lambda u)v \tag{42}$$

Taking Equation 38 to the $-\lambda$ power, and substituting $\cos\alpha = u$ and $\rho_j/r = v$, the below equation can be obtained:

$$\frac{1}{r_j^{2\lambda}} \approx \frac{1}{r^{2\lambda}} \left(1 + 2\lambda \left(-\frac{x_j}{\rho_j}\right)\left(\frac{\rho_j}{r}\right)\right) = \frac{1}{r^{2\lambda}} \left(1 - \frac{2\lambda x_j}{r}\right) \tag{43}$$

As λ is simply a constant that helps to define the Gegenbauer polynomials, it is thus possible to choose values that are convenient for the purpose of linearizing the follower dynamics. Thus, setting $\lambda = 3/2, 5/2$, and $7/2$, expressions for powers of $1/r_j$ in terms of r and x_j can be obtained:

$$\begin{aligned} \frac{1}{r_j^3} &\approx \frac{1}{r^3} - \frac{3x_j}{r^4} \\ \frac{1}{r_j^5} &\approx \frac{1}{r^5} - \frac{5x_j}{r^6} \\ \frac{1}{r_j^7} &\approx \frac{1}{r^7} - \frac{7x_j}{r^8} \end{aligned} \tag{44}$$

Substituting Equations 44 into Equations 37 and removing higher order terms, the following equation is obtained:

$$\begin{aligned}\zeta_j &\approx \zeta - \frac{8k_{J2}x_j s(I)s(\theta)}{r^5} + \frac{2k_{J2}y_j s(I)c(\theta)}{r^5} + \frac{2k_{J2}z_j c(I)}{r^5} \\ \eta_j^2 &\approx \eta^2 - \frac{3\mu x_j}{r^4} - \frac{5k_{J2}x_j(1-5s^2(I)s^2(\theta))}{r^6} - \frac{5k_{J2}y_j s^2(I)s(2\theta)}{r^6} - \frac{5k_{J2}z_j s(2I)s(\theta)}{r^6}\end{aligned} \tag{45}$$

Substituting Equations 45 into Equations 35, the linearized equations of motion for the follower satellite can be obtained, as shown below:

$$\begin{aligned}\ddot{x}_j = \; & 2\dot{y}_j\omega_z + x_j\left(2\eta^2 + \omega_z^2 + \frac{2k_{J2}}{r^5}(1-s^2(I)s^2(\theta)\right) \\ & + y_j\left(\alpha_z + \frac{4k_{J2}s^2(I)s(2\theta)}{r^5}\right) - 5z_j\omega_x\omega_z \\ \ddot{y}_j = & -2\dot{x}_j\omega_z + 2\dot{z}_j\omega_x + x_j\left(\frac{4k_{J2}s^2(I)s(2\theta)}{r^5} - \alpha_z\right) \\ & - y_j\left(\frac{2k_{J2}s^2(I)c^2(\theta)}{r^5} + \eta^2 - \omega_z^2 - \omega_x^2\right) \\ & + z_j\left(\alpha_x - \frac{k_{J2}s(2I)c(\theta)}{r^5}\right) \\ \ddot{z}_j = & -2\dot{y}_j\omega_x - 5x_j\omega_x\omega_z - y_j\left(\frac{k_{J2}s(2I)c(\theta)}{r^5} + \alpha_x\right) \\ & - z_j\left(\eta^2 - \omega_x^2 + \frac{2k_{J2}c^2(I)}{r^5}\right)\end{aligned} \tag{46}$$

Because the above equations are linear, they can be expressed in the form of Equation 47

$$\frac{d}{dt}\begin{bmatrix}\dot{x}_j \\ \dot{y}_j \\ \dot{z}_j\end{bmatrix} = A_1(t)\begin{bmatrix}\dot{x}_j \\ \dot{y}_j \\ \dot{z}_j\end{bmatrix} + A_2(t)\begin{bmatrix}x_j \\ y_j \\ z_j\end{bmatrix} \tag{47}$$

where

$$A_1(t) = \begin{bmatrix}0 & 2\omega_z & 0 \\ -2\omega_z & 0 & 2\omega_x \\ 0 & -2\omega_x & 0\end{bmatrix} \tag{48}$$

and

$$A_2(t) = \begin{bmatrix}2\eta^2 + \omega_z^2 + \frac{2k_{J2}}{r^5}(1-s^2(I)s^2(\theta)) & \alpha_z + \frac{4k_{J2}s^2(I)s(2\theta)}{r^5} & -5\omega_x\omega_z \\ \frac{4k_{J2}s^2(I)s(2\theta)}{r^5} - \alpha_z & \frac{2k_{J2}s^2(I)c^2(\theta)}{r^5} + \eta^2 - \omega_z^2 - \omega_x^2 & \alpha_x - \frac{k_{J2}s(2I)c(\theta)}{r^5} \\ -5\omega_x\omega_z & \frac{k_{J2}s(2I)c(\theta)}{r^5} + \alpha_x & \eta^2 - \omega_x^2 + \frac{2k_{J2}c^2(I)}{r^5}\end{bmatrix} \tag{49}$$

Simulation Results

Validation with STK

We will be validating our nonlinear model with Systems Tool Kit (STK) from AGI. The initial conditions we used in Cartesian are:

$$x_0 = \begin{bmatrix} 6321.118\ km & 2161.574\ km & 1259.871\ km & -3.109\ km/s & 6.791\ km/s & 3.741\ km/s \end{bmatrix}^T$$

and in hybrid elements:

$$x_0 = [6696.779\ km \quad -0.138\ km/s \quad 54440.626\ km^2/s \quad 0.345\ rad \quad 0.513\ rad \quad 0.020\ rad$$
$$100\ km \quad 100\ km \quad 100\ km \quad 0.1\ km/s \quad 0.1\ km/s \quad -0.1\ km/s]^T$$

where the first column represents initial conditions for the Leader in hybrid elements and the second column represents initial conditions for the follower in LVLH frame. The results are given below.

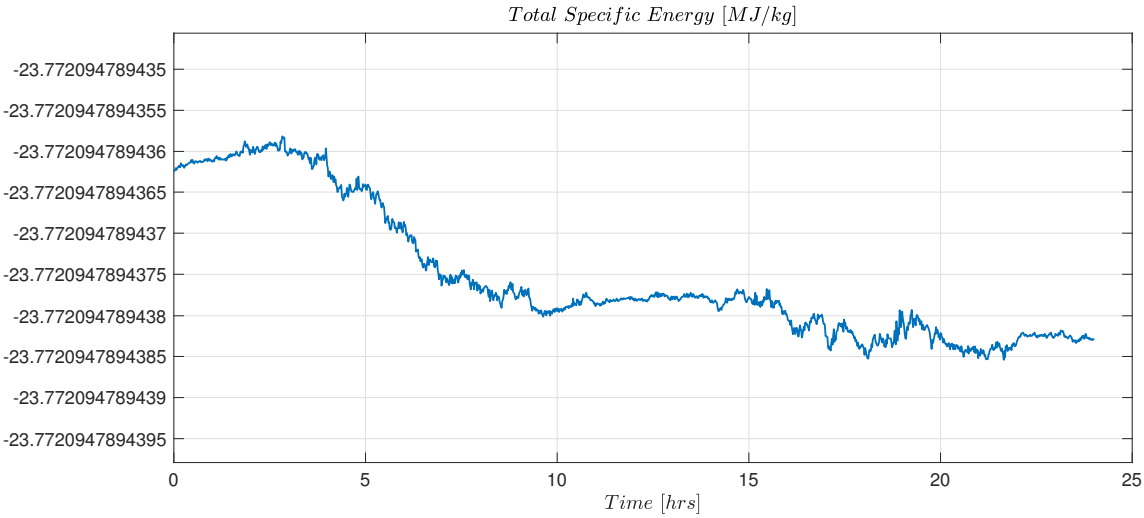

Figure 2: Conservation of Energy

As shown in Figure 2, the conservation of energy is maintained with high accuracy. Furthermore:

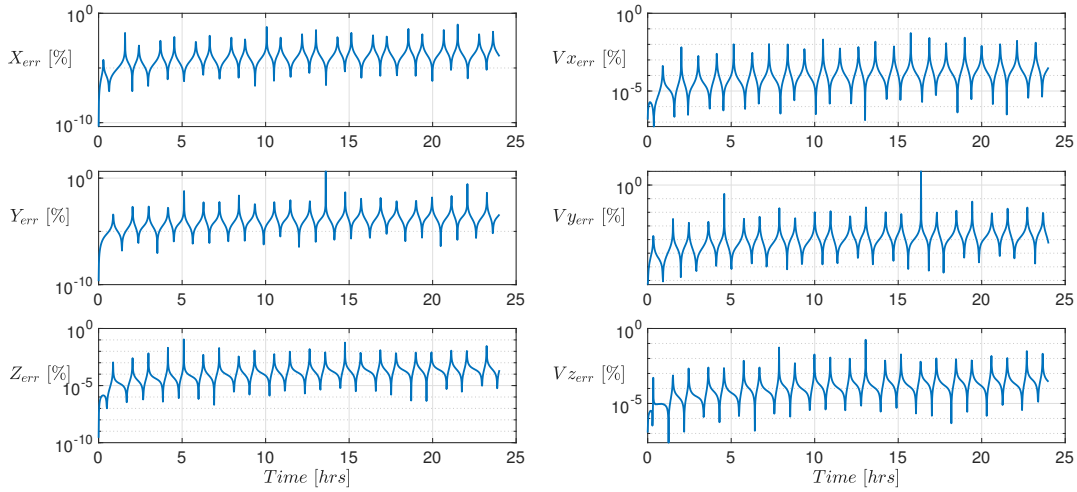

Figure 3: Relative Error

As shown in Figure 3, the relative error of position and velocity in ECI between the STK solution and the nonlinear model hover at around $1e-4$ and $1e-5$ percent. For reference, the STK solution used the Runge-Kutta-Fehlberg 7th and 8th order integrator while we used MATLAB's ode45 integrator. The orbit in ECI frame looks like this:

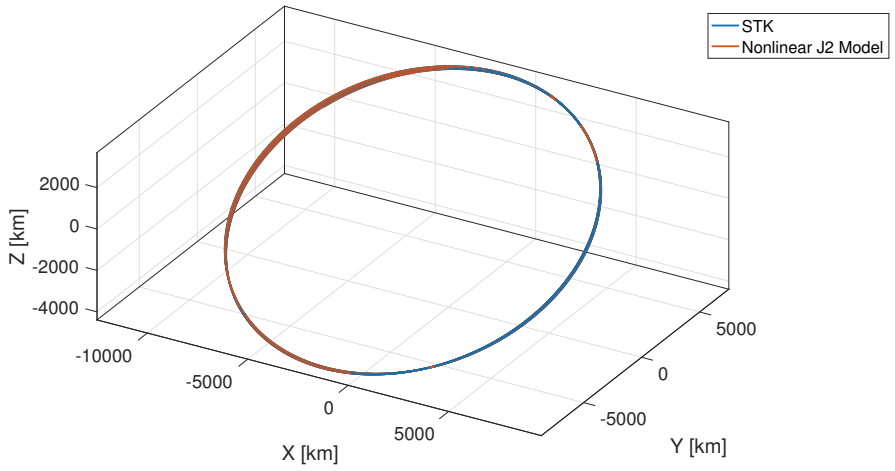

Figure 4: Example Orbit

Comparison between Nonlinear and Linear Models

We now compare the effectiveness of the linear model we derived earlier with our exact J2 nonlinear model. With a low perigee, non-circular orbit with initial conditions:

$$x_0 = [6696.779\ km \quad -0.138\ km/s \quad 54440.626\ km^2/s \quad 0.345\ rad \quad 0.513\ rad \quad 0.020\ rad$$
$$0.001\ km \quad 0\ km \quad 0\ km \quad 0\ km/s \quad 0\ km/s \quad 0\ km/s]^T$$

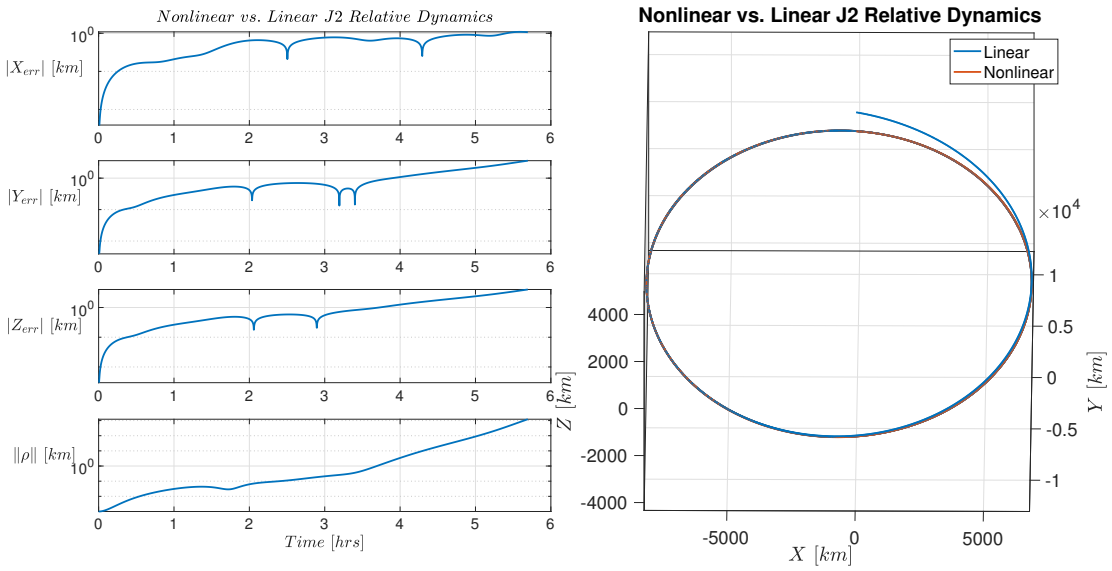

Figure 5: Nonlinear vs. Linear Comparison 1

As one can see in Figure 5, certain initial conditions can cause the relative vector, ρ, for a follower satellite to grow without bounds. Since the linear model we derived is only accurate for small ρ, large ρ will cause the linear model to diverge fairly quickly (1 hour in this case). In contrast, for a high perigee orbit with initial conditions:

$$x_0 = [2000\ km \quad 0\ km/s \quad 8928.611\ km^2/s \quad 0\ rad \quad 0.436\ rad \quad 0\ rad$$
$$0\ km \quad 0.5\ km \quad 0\ km \quad 0\ km/s \quad 0\ km/s \quad 0\ km/s]^T$$

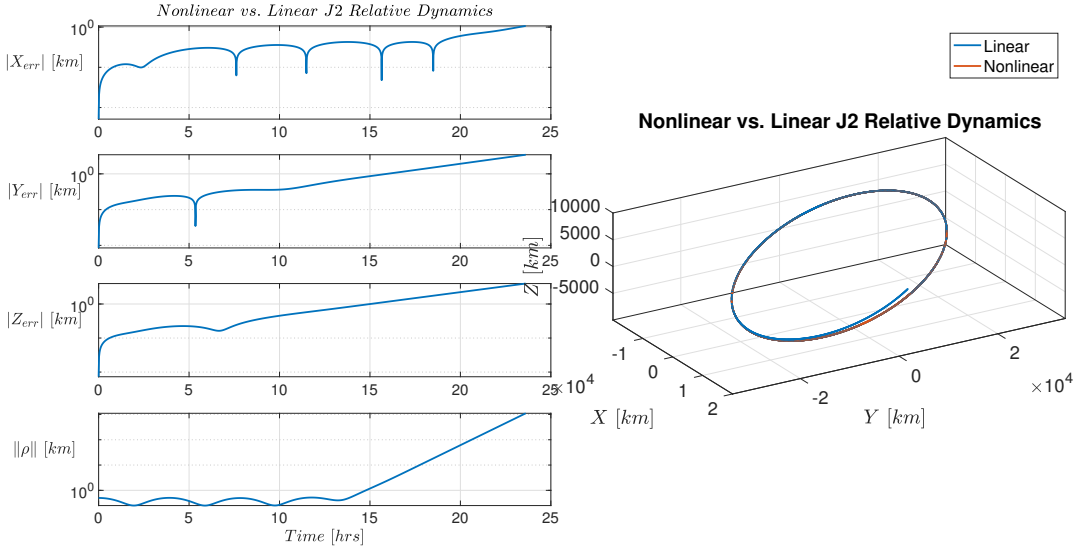

Figure 6: Nonlinear vs. Linear Comparison 2

If ρ is bounded or quasi-periodic, the linear model will be valid for much longer (15x longer than before in this case). Practically, the linear model is still useful to derive linear controllers and state estimators. Furthermore, with regular updates from say, a Kalman filter, the linear model can be used to propagate the orbit after estimation updates.

Finding Quasi-Periodic Relative Orbits

Just a reminder, the Clohessy-Wiltshire equations have the following form:

$$\begin{aligned} \ddot{x} - 2n\dot{y} - 3n^2 x &= f_x \\ \ddot{y} + 2n\dot{x} &= f_y \\ \ddot{z} + n^2 z &= f_z \end{aligned} \tag{50}$$

With zero forcings, the analytical form can be obtained as:

$$\begin{aligned} x(t) &= 4x_0 - 3x_0\cos(nt) + \frac{\dot{x}_0}{n}\sin(nt) + 2\frac{\dot{y}_0}{n} - 2\frac{\dot{y}_0\cos(nt)}{n} \\ y(t) &= -6x_0 nt + 6x_0\sin(nt) + 2\cos(nt)\frac{\dot{x}_0}{n} - 2\frac{\dot{x}_0}{n} + \frac{\dot{y}_0}{n}\left(4\sin(nt) - 3nt\right) + y_0 \\ z(t) &= z_0\cos(nt) + \frac{\dot{z}_0}{n}\sin(nt) \end{aligned} \tag{51}$$

This is very powerful for a mission design perspective because one can fairly easy compute the relative initial conditions for a desired closed-trajectory for a specific mission. Unfortunately, we cannot do so for our exact nonlinear J2 relative dynamics. Even with the linearized model, it is still time varying with respect to the leader's orbital elements. One way to find quasi-periodic orbits for the nonlinear model is to use numerical optimization. More specifically we optimize over the variables:

$$\begin{bmatrix} x_0 & y_0 & z_0 & \dot{x}_0 & \dot{y}_0 & \dot{z}_0 & \cdots & \dot{z}_n & T \end{bmatrix}$$

We are essentially optimization over the relative initial conditions for n follower satellites as well as the period T. The user supplies a function that uses the provided initial conditions to integrate the nonlinear model for duration T. The function then computes a cost function based on the desired orbit characteristics. For instance, one cost function might be a orbit-closure constraint for orbit period T:

$$J = \|state(0) - state(T)\|_2$$

Another good cost function might be total specific energy equality constraint between the leader and follower satellites:

$$J = \|K + U - K_j - U_j\|_2$$

If a circular follower orbit in LVLH frame is desired, then the cost function could be:

$$J = r_{desired} - \left\| \begin{bmatrix} x_0 \\ y_0 \\ z_0 \end{bmatrix} \right\|_2$$

The optimizer will then use function evaluations to find a set of initial conditions that locally minimizes the cost function. Optimizers such as fminunc, fminsearch, or lsqnonlin from MATLAB can be used for this purpose. All furhter simulations are simulated for the duration of 111 hours. One result is the following:

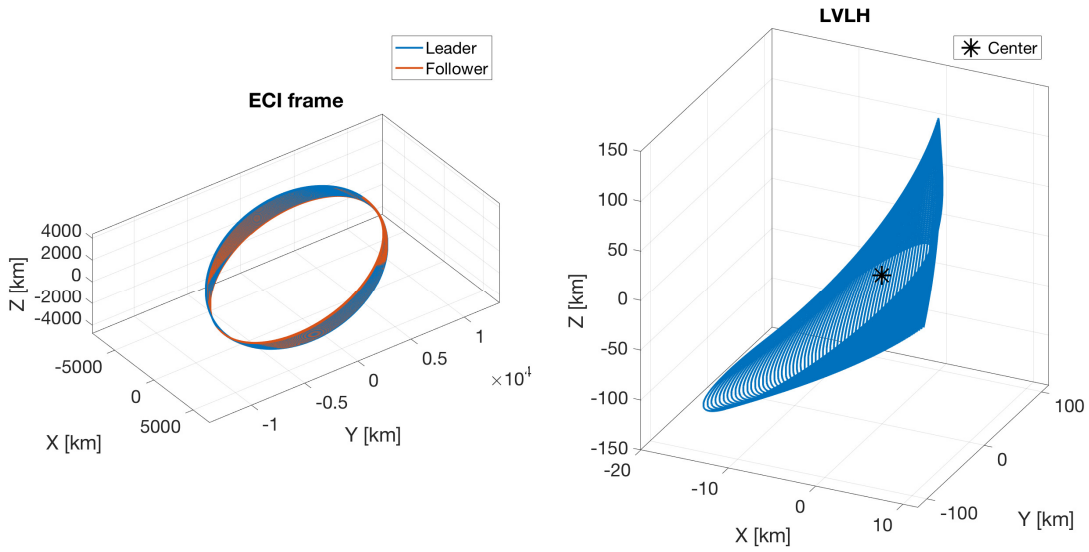

Figure 7: Quasi-Periodic Orbit 1

As shown in Figure 7, there is significant drift in follower relative trajectory. This is disadvantageous because there would need regular thruster firings for station-keeping, which is bad since fuel is an expendable resource. We can do better with the following:

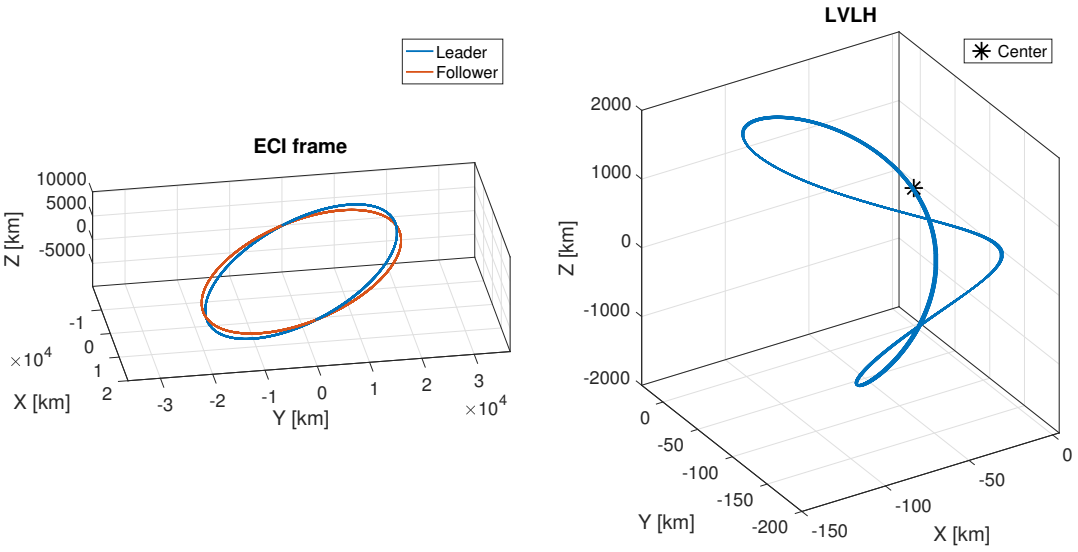

Figure 8: Mirror Orbit

As shown in Figure 8, the follower relative trajectory is actually pretty periodic at least for the simulation duration. The range in Z is large, which can be easily seen due to the slight inclination of the leader orbit from the follower orbit in ECI frame. The relative trajectory is pretty constrained in the LVLH x-y plane. One interesting note is the following simulation with the same initial conditions as Figure 8 but with no J2 effects.

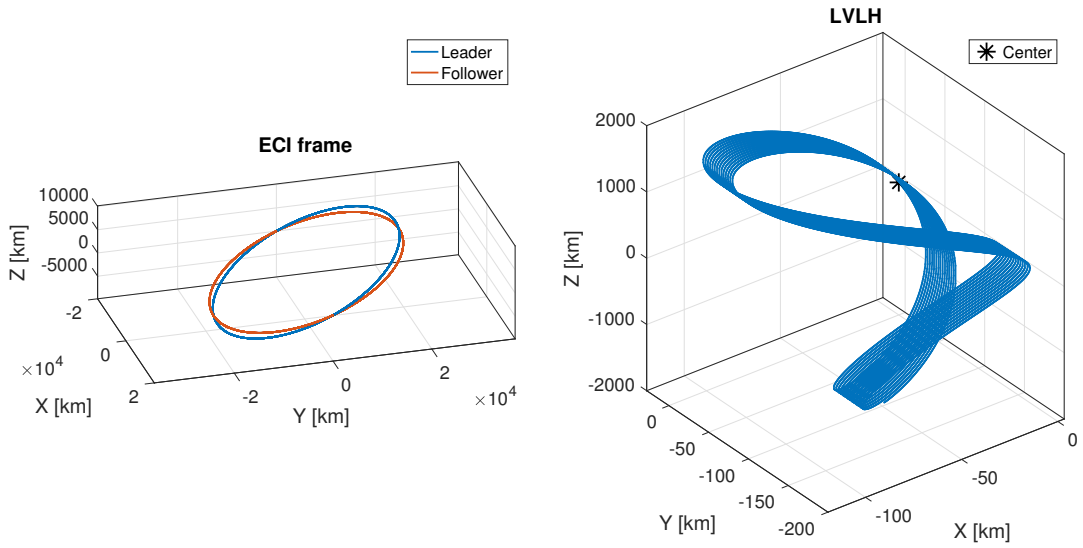

Figure 9: Mirror Orbit no J2

Surprisingly, there is more drift in relative trajectory for the no-J2 case than the J2 case for this particular set of initial conditions. This demonstrates the power of utilizing J2-effects to one's advantage to minimize drift in LVLH frame. Last but not least, we have the following:

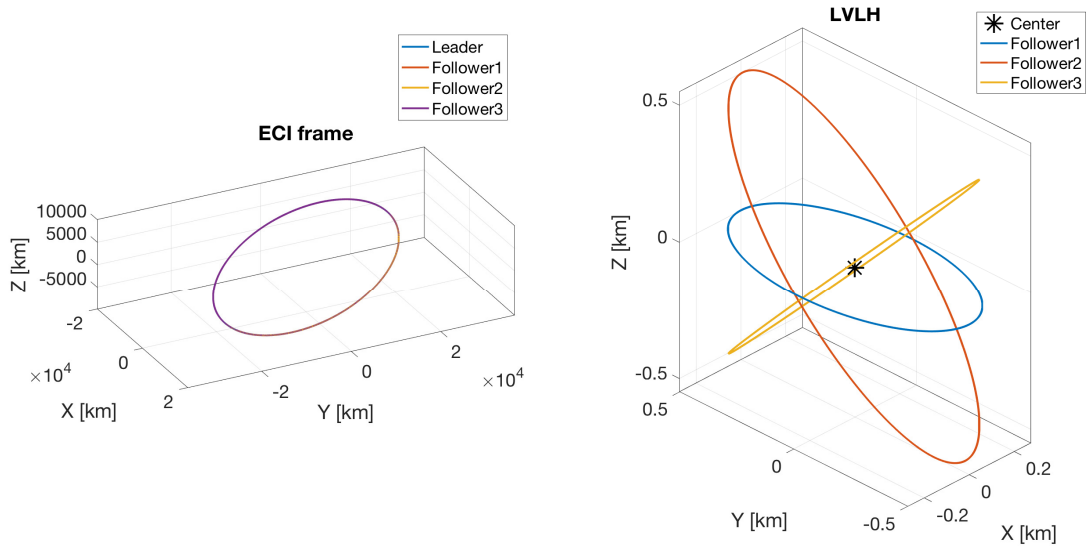

Figure 10: Three Followers

As shown in Figure 10, the three followers' relative orbits in LVLH frame resemble ellipses. The blue ellipse has a semi-major axis of 0.5 km while the yellow and red ellipses have semi-major axes of $0.5\sqrt{2}$ km. The periods of the follower relative orbits as well as the leader orbit around Earth are optimized to be around 7.8 $hours$. Note the follower orbit has no physical meaning (besides it bears the shape of an ellipse) and the ellipse is centered on the leader satellite. For your reference, the initial conditions are:

$$
\begin{aligned}
x_0 = [&2000\ km \quad 0\ km/s \quad 8928.611\ km^2/s \quad 0\ rad \quad 0.436\ rad \quad 0\ rad \\
&0\ km \quad 0.5\ km \quad 0\ km \quad 0.000056\ km/s \quad 0\ km/s \quad 0\ km/s \\
&0.0000219\ km \quad 0.5\ km \quad 0.5\ km \quad 0.000055235\ km/s \quad 0\ km/s \quad 0.000004666\ km/s \\
&0.0000219\ km \quad 0.5\ km \quad -0.5\ km \quad 0.000055236\ km/s \quad -0.00000001078\ km/s \quad 0.00000466\ km/s]^T
\end{aligned}
$$

The first column represents the initial conditions for the leader satellite while the next three columns represent the relative initial conditions for the follower satellites

Conclusion

In summary, we have derived exact nonlinear relative dynamics with J2 effects. We further linearized the nonlinear dynamics for small relative vectors. We validated our nonlinear model with STK. We also showed the effectiveness of the linear model for small relative vectors. Finally, we used numerical optimization techniques to search for initial conditions that can create quasi-periodic orbits.

References

References

[1] Wang, D., Wu, B. and Poh, E. (2017). *Satellite Formation Flying*. Singapore: Springer Singapore.

[2] Xu, G. and Wang, D. (2008). Nonlinear Dynamic Equations of Satellite Relative Motion Around an Oblate Earth. *Journal of Guidance, Control, and Dynamics*, 31(5), pp.1521-1524.

[3] Liu, G. and Zhang, S. (2018). A Survey on Formation Control of Small Satellites. *Proceedings of the IEEE*, 106(3), pp.440-457.